

Dual inhibition of PI3K and mTOR inhibits autocrine and paracrine proliferative loops in PI3K/Akt/mTOR-addicted lymphomas

*Aadra P. Bhatt,¹ *Prasanna M. Bhende,¹ Sang-Hoon Sin,¹ Debasmitta Roy,¹ Dirk P. Dittmer,¹ and Blossom Damania¹

¹Lineberger Comprehensive Cancer Center and Department of Microbiology & Immunology, University of North Carolina at Chapel Hill

Primary effusion lymphoma (PEL) constitutes a subset of non-Hodgkin lymphoma whose incidence is highly increased in the context of HIV infection. Kaposi sarcoma-associated herpesvirus is the causative agent of PEL. The phosphatidylinositol 3-kinase (PI3K) signaling pathway plays a critical role in cell proliferation and survival, and this pathway is dysregulated in many different cancers, including PEL, which display activated PI3K, Akt, and mammalian target of rapamycin (mTOR) kinases. PELs

rely heavily on PI3K/Akt/mTOR signaling, are dependent on autocrine and paracrine growth factors, and also have a poor prognosis with reported median survival times of less than 6 months. We compared different compounds that inhibit the PI3K/Akt/mTOR pathway in PEL. Although compounds that modulated activity of only a single pathway member inhibited PEL proliferation, the use of a novel compound, NVP-BEZ235, that dually inhibits both PI3K and mTOR kinases was significantly more efficacious in culture

and in a PEL xenograft tumor model. NVP-BEZ235 was effective at low nanomolar concentrations and has oral bioavailability. We also report a novel mechanism for NVP-BEZ235 involving the suppression of multiple autocrine and paracrine growth factors required for lymphoma survival. Our data have broad applicability for the treatment of cytokine-dependent tumors with PI3K/mTOR dual inhibitors. (*Blood*. 2010;115(22):4455-4463)

Introduction

The phosphatidylinositol 3-kinase (PI3K) signaling pathway plays a critical role in cell proliferation and cell survival. PI3K activation stimulates the production of phosphatidylinositol 3,4,5-triphosphate, which results in activation of the kinases PDK1 and Akt. The lipid phosphatase and tensin homolog deleted on chromosome 10 (PTEN) protein is a negative regulator of this pathway. Akt kinase promotes cell survival by phosphorylating, and thereby inactivating, proapoptotic factors, such as the FOXO transcription factor family, GSK-3 β , caspase-9, and Bad.¹⁻⁴ Phosphorylation of Bad and the FOXO transactivators prevent apoptosis. Akt also phosphorylates p27, a negative regulator of the cell cycle, thereby preventing cell cycle arrest. In addition, Akt activation leads to phosphorylation and activation of the mammalian target of rapamycin (mTOR), a kinase that stimulates protein synthesis and cell proliferation.

Activated mTOR protein can associate with raptor and mLST8/G β L to form the mTORC1 complex. The mTORC1 complex induces phosphorylation of p70 S6 kinase (S6K), leading to phosphorylation and activation of the ribosomal protein S6. mTORC1 also inhibits 4E-BP1, a repressor of eukaryotic initiation factor eIF4E. This arm of the mTOR pathway is rapamycin-sensitive. In contrast, the mTORC2 complex, which consists of mTOR, mLST8/G β L, mSin1, and Rictor, is insensitive to the effects of rapamycin. mTORC2 functions in a feedback loop that phosphorylates and activates Akt by phosphorylation at Ser473.⁵ Hence, inhibitors of PI3K/Akt probably have broader effects than mTOR inhibitors.

The nutrient sensor, AMP activated kinase (AMPK), is a negative regulator of mTORC1.⁶ AMPK controls cellular homeostasis by regulating energy production within the cell. AMPK is activated when the cellular AMP/adenosine triphosphate (ATP)

balance drops, and this leads to activation of fatty acid oxidation in the liver, lipogenesis, stimulation of ketogenesis, and inhibition of cholesterol synthesis. The net result of modulation of these pathways is the inhibition of mTOR, which results in attenuation of protein synthesis until cellular ATP reserves are sufficiently replenished. The glitazone class of drugs is known to activate AMPK,^{7,8} leading us to hypothesize that AMPK activation may be of therapeutic value in treating mTOR-addicted lymphomas. In addition, AMPK activation has previously been shown to inhibit some tumor types.^{8,9}

We chose primary effusion lymphoma (PEL) as the target for our investigation because PELs rely heavily on PI3K/Akt/mTOR signaling¹⁰ and have a very poor prognosis, with reported median survival times of less than 6 months.¹¹ PEL is a variant of non-Hodgkin lymphoma (NHL) and is infected with Kaposi sarcoma associated-herpesvirus (KSHV). KSHV is associated with multiple cancers in the human population; Kaposi sarcoma (KS), PEL, and multicentric Castleman disease. The incidence of these cancers is highly increased in the context of HIV infection. We, and others, have previously shown that individual viral proteins, such as KSHV K1, activate the PI3K/Akt pathway in B cells and endothelial cells.¹²⁻¹⁶ Another viral protein, KSHV vGPCR, can also activate this pathway in endothelial and epithelial cells.¹⁷⁻²¹ KSHV-infected PELs display constitutive activation of the PI3K/Akt/mTOR pathway.¹⁰ No activating PI3K mutations have been reported in PEL, and only 2 PEL lines display PTEN mutations.²² This suggests that in PEL constitutive activation of PI3K, Akt, and mTOR kinases is the result of the expression of viral proteins. We previously reported that treatment with rapamycin, an mTOR

Submitted October 28, 2009; accepted February 19, 2010. Prepublished online as *Blood* First Edition paper, March 18, 2010; DOI 10.1182/blood-2009-10-251082.

*A.P.B. and P.M.B. contributed equally to this study.

The online version of this article contains a data supplement.

The publication costs of this article were defrayed in part by page charge payment. Therefore, and solely to indicate this fact, this article is hereby marked "advertisement" in accordance with 18 USC section 1734.

© 2010 by The American Society of Hematology

inhibitor, induces cell cycle arrest in PEL and may halt clinical progression.¹⁰ Rapamycin inhibits mTORC1, but not mTORC2. However, recent literature suggests that there is increased mTORC2-mediated phosphorylation of Akt, which compensates for mTORC1 inhibition by rapamycin, in some cell types and tumors.²³ Hence, single-agent rapamycin therapy has had limited success in the clinic.

Here, we report the consequences of modulating Akt and AMPK kinases individually, as well as simultaneously inhibiting PI3K and mTOR kinases in PEL. All the compounds tested are either already Food and Drug Administration-approved or currently in clinical trials. We demonstrate that dual inhibition of PI3K and mTOR with a novel, orally bioavailable compound, NVP-BEZ235, is more efficacious than single compounds in preventing PEL proliferation and tumor growth in mice. We are the first to report that one mechanism of action for NVP-BEZ235 involves the inhibition of autocrine and paracrine cytokine and growth factors, which may explain the heightened sensitivity of cytokine driven cancers to inhibitors of the PI3K/Akt/mTOR pathway.

Methods

Cell culture

Patient-derived, PEL cell lines (BC-1, BCBL-1, BCLM, BCP-1, and VG-1) were cultured in RPMI 1640 supplemented with 10% heat-inactivated fetal bovine serum, 100 IU/mL penicillin G, 100 µg/mL streptomycin (Mediatech), 0.075% sodium bicarbonate, and 0.05mM β-mercaptoethanol (Invitrogen) at 37°C in 5% CO₂. BC-1 is EBV(+)/KSHV(+), whereas the other cell lines are KSHV(+).

Inhibitors

Perifosine, miltefosine, and rosiglitazone were purchased from Cayman Chemical. Ciglitazone was purchased from Calbiochem. We are grateful to Novartis for providing us with NVP-BEZ235.

MTS cell proliferation assay

To observe alterations in growth and proliferation, 2×10^5 PEL cells were treated with the therapeutic compounds at the indicated doses or with appropriate vehicle as a negative control. Cells were followed for 96 hours, and cell viability was determined by trypan blue exclusion performed in quadruplicate. Actively metabolic cells were quantified every 24 hours using the Cell Titer 96 Aqueous One Solution Cell Proliferation Assay (Promega) according to the manufacturer's instructions. Absorbance was measured using FLUOstar OPTIMA (BMG Labtech). The absorbance measured at 485 or 490 nm indicates the number of metabolically active cells. The 50% inhibitory concentration (IC₅₀) of NVP-BEZ235 was calculated by plotting the percentage inhibition in proliferation in NVP-BEZ235-treated cells compared with vehicle-treated cells (y-axis) versus the log of the concentration of drug (x-axis). This was done using the statistical analysis program R. The dose of NVP-BEZ235 that reduced cell proliferation to 50% of vehicle-treated cells was calculated as the IC₅₀ for NVP-BEZ235.

Western blots

Cells were treated with various compounds as indicated. After washing harvested cells with ice-cold phosphate-buffered saline (PBS), cell lysates were prepared in a buffer containing 150mM NaCl, 50mM Tris-HCl (pH 8), 0.1% NP40, 50mM NaF, 30mM β-glycerophosphate, 1mM Na₃VO₄, and 1× Complete Protease Inhibitor cocktail (Roche Diagnostics). Equal amounts of proteins were electrophoresed on a 10% sodium dodecyl sulfate-polyacrylamide gel electrophoresis denaturing gel, followed by transfer onto a Hybond-ECL nitrocellulose membrane (GE Healthcare). Membranes were blocked with 5% fat-free milk for 1 hour at room

temperature, followed by overnight incubation at 4°C in the indicated primary antibodies directed against either phosphorylated or total protein. The following primary antibodies against phosphorylated proteins were used: AMPKα (Thr172), Akt (Ser473), Akt (Thr308), FOXO1 (Ser256), GSK3β (Ser9), mTOR (Ser2448), S6K (Thr421/Ser424), and S6 ribosomal protein (Ser235/236). After washing, the membrane was incubated with anti-rabbit IgG conjugated to horseradish peroxidase. The results were visualized with the ECL Plus Western Blotting Detection System (GE Healthcare) according to the manufacturer's instructions.

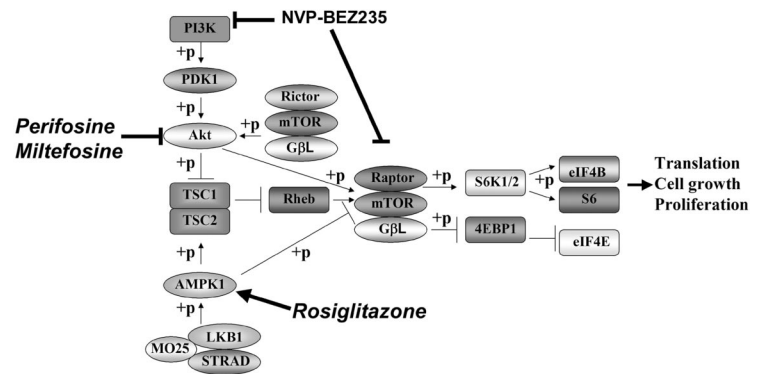
Xenograft tumor model

PEL cells were washed in ice-cold phosphate buffered saline (Mediatech), counted, and diluted in 100 µL of PBS mixed with 100 µL of growth factor-depleted Matrigel (BD Biosciences).¹⁰ A total of 1×10^5 to 7.5×10^5 BC-1 cells were injected subcutaneously into the right flank of NOD.CB17-Prkdc^{scid}/J or CB17-Prkdc^{scid}/J mice (The Jackson Laboratory, Taconic Farms). The mice were monitored on alternate days for development of palpable tumors (~2 mm³), at which point drug or vehicle treatments were initiated, and were administered either intraperitoneally (perifosine) or by oral gavage (rosiglitazone, NVP-BEZ235) 5 days a week. Groups of 5 to 7 mice were used to generate PEL tumors and treated with either vehicle or drug cocktail. Each biologic experiment was repeated multiple times. For rosiglitazone, 0.25% methylcellulose was used as vehicle, and 30 mg/kg or 60 mg/kg rosiglitazone was suspended in methylcellulose. For perifosine and miltefosine, PBS was used as a vehicle and 50 mg/kg perifosine or miltefosine was dissolved in PBS. For NVP-BEZ235, the compound was dissolved in a 1:9 vol/vol mixture of 1-methyl-2-pyrrolidone (Fluka) and polyethylene glycol 300 (Sigma-Aldrich). A dose of 40 mg/kg NVP-BEZ235 or equal volume of the vehicle was administered. Tumor diameters were measured using digital calipers, and tumor volume was calculated as volume = $a \times b \times [\text{MAX}(a, b)]/2$, with a and b being the long and short diameters of the tumor, respectively. The tumors were excised and fixed in formalin. Statistical analyses were performed using linear model fit by maximum likelihood with individual animals treated as random effect.²⁴

Immunohistochemistry

Tumors were excised, fixed in 10% neutral buffered formalin for 5 days, were paraffin-embedded and then 5-µm sections were prepared on slides. Slides were deparaffinized using Histochoice Clearing Agent (Sigma-Aldrich) and rehydrated using graded ethanol, followed by extensive washing with water. Endogenous peroxidase activity was quenched with 3% H₂O₂ in 10% methanol solution, and antigens were exposed by heating sections for 10 minutes in 1mM ethylenediaminetetraacetic acid (pH 8.0), and cooled to room temperature. Nonspecific antigens were blocked using a blocking buffer (10% normal horse serum [Vector Labs], 5% bovine serum albumin [Sigma-Aldrich], and 0.3% Triton X-100) for 1 hour at room temperature, followed by an overnight incubation at 4°C in blocking buffer containing the indicated antibodies: phospho-AMPK (Thr172, 1:50), phospho-p70 S6 kinase (Thr421/Ser424, 1:50), phospho-Akt (Ser473, 1:50), and phospho-S6 (Ser235/236, 1:100), all from Cell Signaling Technology. Sections incubated in blocking buffer lacking primary antibody were used as negative controls. The next day, sections were washed in PBS, incubated with biotinylated goat anti-rabbit secondary antibody followed by 1-hour incubation in preformed Avidin DH-biotinylated horseradish peroxidase H complexes (Vectastain ABC kit, Vector Labs), after which sections were stained with Vector NovaRed substrate and washed. Sections were counterstained with hematoxylin (Invitrogen), dehydrated using graded alcohols, and mounted using Cytoseal XYL (Richard-Allan Scientific). Dried slides were imaged using a Leica DM LA histology microscope with a 10×/0.25 numeric aperture (NA) or 40×/0.75 NA objective using a Leica DPC 480 camera and associated Leica Firecam software on a Macintosh computer equipped with OS X 10.4. Images were stored as .tif files and image layout was processed using Adobe Photoshop CS.

Figure 1. Schematic representation of cellular pathways leading to cell survival or cell death. The roles PI3K, Akt, and AMPK play in signaling pathways important for cell survival or cell death are shown. The influence of rosiglitazone, miltefosine, perifosine, and NVP-BE235 on these pathways is also shown. Phosphorylation of proteins is indicated by “+p.”



Caspase-3 assay

Levels of enzymatically active caspase-3 were quantified using the ApoAlert Caspase Fluorescent assay kit (Clontech), according to the manufacturer's directions. Briefly, 1×10^6 BC-1 PEL cells were treated with 50 μ M miltefosine, 50 μ M perifosine, or 20 nM NVP-BE235, as well as the respective vehicle controls. Cells were harvested and lysed 12 hours later. Equivalent micrograms of cell lysate for all samples were incubated with a fluorogenic caspase-3 substrate (DEVD-AFC). Cleavage of DEVD by caspase-3 releases AFC, the fluorescence of which was measured using a FLUOstar OPTIMA (BMG Labtech) fluorometer, with excitation and emission filter wavelengths set to 400 and 505 nm, respectively.

Cytokine measurements

We measured the levels of 30 different cytokines in the growth medium supernatants of BC-1 PEL cells using a bead-based multianalyte bead immunoassay (Invitrogen Cytokine human 30-plex panel) according to the manufacturer's guidelines. Briefly, diluted (1:2) culture supernatants were incubated with internally dyed polystyrene beads coated with specific antibodies directed against one of the cytokines. Proteins in the culture supernatants bind to the antibody-coated beads during a 2-hour incubation, after which the beads are washed extensively. Biotinylated detector antibodies directed against specific proteins are added to the beads, where they bind to proteins derived from culture supernatants. After washing, streptavidin-conjugated R-phycoerythrin was added to the bead-culture supernatant derived protein-detector antibody complexes. Unbound streptavidin-conjugated R-phycoerythrin was washed off, and the bead complexes were analyzed using the Luminex Detection system. Cytokine concentrations in culture supernatants were extrapolated based on a standard curve generated using manufacturer-supplied standards of each cytokine analyte.

Results

We used several compounds that are either Food and Drug Administration–approved or in clinical trials to target multiple arms of the PI3K/Akt/mTOR pathway (Figure 1). The glitazone class of drugs, eg, ciglitazone and rosiglitazone, have been shown to activate AMPK.^{7,8} Activated AMPK1 directly phosphorylates and activates TSC2,^{25,26} leading to inactivation of Rheb and mTOR. We also used perifosine and miltefosine, 2 alkylphospholipids, which have been shown to inhibit Akt.²⁷ Perifosine is currently in clinical trials for solid tumors.²⁸ Lastly, we evaluated a novel, orally bioavailable, dual inhibitor of PI3K and mTOR (Figure 1), NVP-BE235.

The glitazones inhibit PEL growth in vitro

Ciglitazone and rosiglitazone are antidiabetic compounds belonging to the thiazolidinedione class of drugs. Both activate AMPK via activation of peroxisome proliferator-activated receptor- γ and

adiponectin.^{7,29,30} To determine the efficacy of ciglitazone and rosiglitazone against PEL, we treated PEL cell lines with either 100 μ M ciglitazone or 150 μ M and 200 μ M rosiglitazone for 96 hours.³¹ Cell viability was measured using the MTS assay. Four different PEL cell lines treated with ciglitazone or rosiglitazone showed decreased viability compared with vehicle (dimethyl sulfoxide [DMSO])–treated cells. Both 100 μ M ciglitazone and 200 μ M rosiglitazone displayed similar growth-inhibitory effects on BCLM and VG-1 (approximately 4- and 5-fold, respectively). The inhibitory effects of ciglitazone were greater on BCLM and VG-1 than on BCBL-1 and BCP-1 (Figure 2). This reduced sensitivity to ciglitazone may be a consequence of *p53* mutations in BCBL-1 and BCP-1,³² which could prevent phosphorylated AMPK from exerting its full inhibitory effect. Indeed, a previous report showed that the stabilization and activation of AMPK induce *p53*-dependent apoptosis.³³ AMPK phosphorylation was increased on treatment of the PEL lines with either 100 μ M ciglitazone or 200 μ M rosiglitazone (Figure 3A), indicating that these compounds activated their target. As expected, there was a corresponding decrease in the phosphorylation of mTOR and its downstream targets, S6K, as well as S6 itself (Figure 3A).

Rosiglitazone delays PEL tumor growth in vivo

To investigate the effect of rosiglitazone on PEL growth in vivo, BC-1 cells were subcutaneously injected into NOD-SCID mice in the presence of growth factor–depleted Matrigel.¹⁰ On development of palpable tumors, the animals were randomized into groups of 5 and treated 5 days a week for the duration of the experiment with either 0.25% methylcellulose (vehicle) or with 30 mg/kg or 60 mg/kg rosiglitazone suspended in methylcellulose via oral gavage similar to previous reports.⁸ The animals were killed after 14 days, and tumors were harvested and measured. Both doses of rosiglitazone delayed tumor growth to some extent (Figure 3B); however, the differences were not statistically significant. Immunohistochemistry showed that AMPK phosphorylation at Thr172 was increased in the rosiglitazone-treated mice compared with vehicle-treated mice (Figure 3C). S6K, a downstream effector of mTOR, was uniformly phosphorylated at Thr421/Ser424 and detectable in tumors in mice treated with the vehicle (methylcellulose) but was virtually undetectable in tumors from mice treated with rosiglitazone (Figure 3C). This suggests that rosiglitazone delays tumor growth via activation of AMPK and inhibition of protein translation through mTOR.

Miltefosine and perifosine target Akt and inhibit proliferation of PEL in vitro

Miltefosine and perifosine are alkylphospholipids that inhibit activation of Akt.²⁷ We treated BCLM, VG-1, BC-1, and BCBL-1

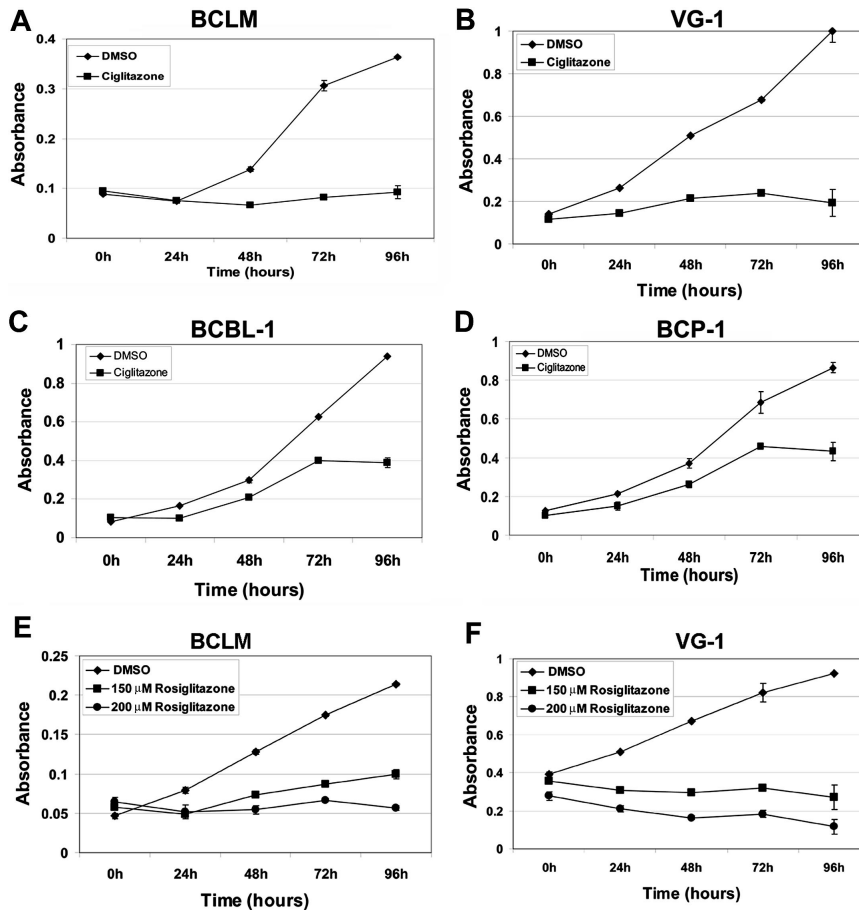


Figure 2. Inhibition of PEL cell proliferation induced by ciglitazone and rosiglitazone as measured by MTS assay. Shown in each panel (y-axis) is the absorbance at 490 nm in vehicle (DMSO) without drug (\blacklozenge) or presence of 100 μ M ciglitazone (A-D, \blacksquare) or 150 μ M (E-F, \blacksquare) or 200 μ M rosiglitazone (E-F, \bullet) versus time in hours after drug treatment (x-axis). Each data point is the average of triplicate or quadruplicate measurements. Error bars represent the SD and in most cases are smaller than the symbol.

PEL cell lines with 10, 20, 30, 40, and 50 μ M miltefosine or perifosine over a 3-day period.^{27,34} Figure 4A shows a representative MTS experiment using the VG-1 cell line and both drugs. Perifosine was a more potent inhibitor of PEL growth compared with miltefosine at all concentrations. Perifosine treatment inhibited Akt and its downstream proapoptotic targets, FOXO1 and GSK-3 β , comparable with the levels of the PI3K inhibitor, LY294002.¹³ The protein translation arm of the Akt pathway was also inhibited, as phosphorylation of mTOR (Ser2448), S6K (Thr421/Ser424), and the S6 ribosomal subunit (Ser235/236) was decreased (Figure 4B).

Miltefosine and perifosine delay PEL tumor progression in vivo

We subcutaneously injected NOD-SCID mice with BC-1 cells suspended in growth factor-depleted Matrigel. On formation of palpable tumors, mice were randomized into groups of 5 and injected intraperitoneally 5 days a week with 50 mg/kg of either miltefosine or perifosine dissolved in PBS, or equivalent volume of vehicle (PBS). Both miltefosine and perifosine inhibited the growth rate of tumors compared with vehicle-treated mice (Figure 4C). By day 14 after treatment, there was an approximately 50% decrease in average tumor volume in perifosine- and miltefosine-treated mice, compared with vehicle-treated mice ($P < .04$). Tumor growth was also significantly retarded ($P < .04$ for perifosine and $P \leq .055$ for miltefosine by linear mixed-effects model analysis). Immunohistochemical analyses (Figure 4D) displayed an overall reduction in staining for phosphorylated ribosomal S6 protein in tumor sections from miltefosine- and perifosine-treated mice compared with the PBS-treated mice. This reduced phosphor-

ylation correlated with the delay in tumor progression in drug-treated animals. Sections that were not incubated with primary antibody showed no phosphorylated S6 staining (Figure 4D).

NVP-BEZ235 treatment inhibits proliferation of PEL cell lines in vitro

NVP-BEZ235 is an imidazo[4,5-c]quinoline derivative compound shown to inhibit PI3K and mTOR kinase activity both in vitro and in vivo.^{35,36} NVP-BEZ235 inhibits the activity of these 2 kinases by binding, reversibly and competitively, to the ATP-binding cleft, thereby preventing phosphorylation and activation of downstream targets.¹⁰ We treated BCBL-1, BC-1, and VG-1 PEL cell lines with either 50 or 100 nM NVP-BEZ235 and compared cell proliferation of drug-treated or mock-treated cells over a 36-hour time period using the MTS assay. Notably BCBL-1 cells show partial resistance to 50 nM rapamycin,¹⁰ yet the same cells remain sensitive to the dual inhibitor. Figure 5A shows representative cell proliferation profiles of the aforementioned PEL cell lines. The concentration of NVP-BEZ235 required for inhibiting PEL cell proliferation by 50% was 5.68 plus or minus 1.76 nM (Figure 5B) for the BC-1 cell line. The low inhibitory concentration of NVP-BEZ235 confirms the usefulness of this compound as a treatment for PEL and suggests a favorable pharmacokinetic profile. We also performed an MTS assay using a combination of 30 μ M perifosine and 50 nM NVP-BEZ235 against PEL (supplemental Figure 1, available on the *Blood* Web site; see the Supplemental Materials link at the top of the online article). As expected, because NVP-BEZ235 inhibits PI3K upstream of Akt, the

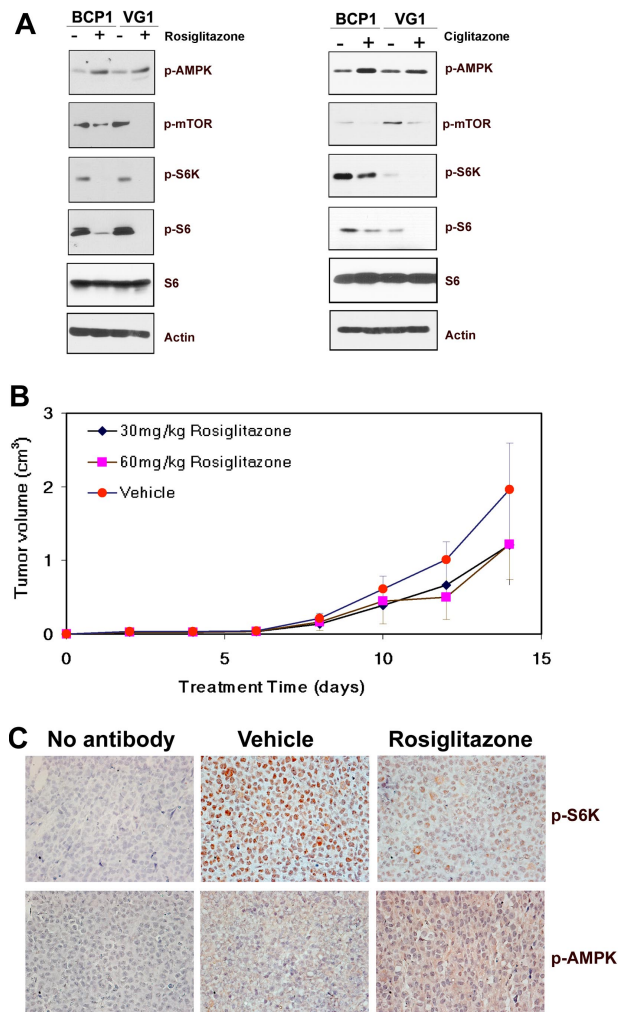


Figure 3. Effect of gliptazone treatment on cellular signaling pathways and tumors in mice. (A) Immunoblot analysis of protein extracts from the indicated cell lines exposed to DMSO (–) or 200 μ M rosiglitazone for 72 hours, or 100 μ M ciglitazone for 96 hours was performed to visualize the expression of phosphorylated AMPK (Ser172), mTOR (Ser 2448), S6K (T421/S424), or S6 (S235/236) proteins along with total S6 and β -actin as loading controls. (B) Decrease in the average tumor size in mice treated with rosiglitazone compared with those treated with methylcellulose (vehicle). Volumes of tumors in mice treated with methylcellulose as vehicle (n = 5), 30 mg/kg rosiglitazone (n = 5), or 60 mg/kg rosiglitazone (n = 5) are plotted on the y-axis versus time in days after inoculation on the x-axis. Error bars represent the SD for each group of animals. (C) Increase in phospho-AMPK (pAMPK; T172) and decrease in phospho-S6K (pS6K; T421/S424) in mouse xenograft tumors on treatment with rosiglitazone. Immunohistochemistry of mouse xenograft tumors using antibodies specific for pAMPK and pS6K is shown. No staining was observed in the absence of a specific primary antibody (no antibody). Original magnification \times 400.

combination of the Akt inhibitor perifosine and NVP-BE2235 did not significantly affect BC-1 proliferation compared with NVP-BE2235 alone.

To confirm the efficacy of NVP-BE2235 against downstream targets of PI3K and mTOR, we tested the phosphorylation status of the downstream targets of these 2 kinases, using Western blot analysis (Figure 5C). Treatment with NVP-BE2235 for 24 hours induced marked reduction in phosphorylated mTOR (Ser2448) and FOXO1 (Ser256), both targets of the kinase activity of PI3K/Akt. Reduced phosphorylation of S6K (Thr421/Ser424) and the ribosomal S6 protein (Ser235/236), both targets of mTOR, reflects inhibition of mTOR by NVP-BE2235. Importantly, reduction in the phosphorylation of Akt at Ser473, a feedback phosphorylation substrate of mTORC2, indicates that NVP-BE2235 also inhibits mTORC2 activity (Figure 5C).¹⁰ Thus, dual inhibition of PI3K and

mTOR likely contributes to decreased cell proliferation by NVP-BE2235.

Dual inhibition of PI3K and mTOR in PEL tumor progression in vivo

We subcutaneously injected NOD-SCID mice with BC-1 PEL cells suspended in growth factor-depleted Matrigel as described in “Methods.” On formation of palpable tumors, mice were randomized to receive either orally administered 40 mg/kg NVP-BE2235 (n = 7) or vehicle (n = 6) 5 days a week. NVP-BE2235 significantly inhibited the growth rate of tumors compared with vehicle-treated mice (Figure 6A). After drug administration, NVP-BE2235-treated mice displayed tumors with significantly smaller volumes compared with vehicle-treated mice ($P < .001$ by linear mixed-effects model analysis). Immunohistochemical analyses of tumors derived from NVP-BE2235-treated mice displayed an overall reduction in staining for phosphorylated ribosomal S6 (Ser235/236) protein and phosphorylated Akt (Ser473), compared with tumors from vehicle-treated mice (Figure 6B). Reduced phosphorylation of the S6 ribosomal protein suggests a reduction in protein translation, leading to delayed tumor progression in NVP-BE2235-treated mice. Reduced phosphorylation of Akt at Ser473 confirms the inhibition of mTOR, which can phosphorylate Akt at Ser473 via the rapamycin-insensitive mTORC2 complex (Figure 6B).

PI3K/Akt inhibition triggers apoptosis in PEL cells

Activation of the PI3K and Akt kinases is important for cell survival. Since the inhibition of PI3K/Akt is known to induce apoptosis, we analyzed the levels of active caspase-3 in PEL cell lines treated with the Akt inhibitors miltefosine or perifosine and the dual inhibitor NVP-BE2235. BC-1 cells were treated with 50 μ M miltefosine, 50 μ M perifosine, 20 nM NVP-BE2235, or their respective vehicle controls for 24 hours. Cells were harvested and equivalent amount of cell lysates were measured for caspase-3 enzymatic activity as a marker of apoptosis. We found that NVP-BE2235-treated BC-1 cells displayed substantially higher levels of activated caspase-3 compared with miltefosine- and perifosine-treated cells (Figure 6C). The enhanced ability of NVP-BE2235 to induce caspase-3-mediated cell death may explain why NVP-BE2235 shows higher activity against PEL in vitro and in vivo. We also performed Trypan blue staining to determine the number of live versus dead cells in PEL treated with 200 μ M rosiglitazone, 50 μ M perifosine, 50 μ M miltefosine, or NVP-BE2235 (10 and 100 nM) at various time points. We found that, after a 24-hour drug treatment, NVP-BE2235 and perifosine were more cytotoxic to PEL cells than rosiglitazone (supplemental Figure 2).

Rosiglitazone, perifosine, and NVP-BE2235 change the cytokine profile of PEL

PELs are highly sensitive to inhibition of autocrine growth factor signaling pathways.³⁷ The cytokines interleukin-6 (IL-6) and IL-10 are particularly important for PEL growth,³⁷ and our group has demonstrated that suppression of IL-6 and IL-10 translation by the mTOR inhibitor rapamycin inhibits PEL cell proliferation. We investigated the cytokine expression levels of the PEL cell line, BC-1, using a 30-plex Luminex bead array (Figure 7). BC-1 PEL cells secrete high amounts of IL-6, IL-10, IP-10/CXCL10, hepatocyte growth factor (HGF), MIG/CXCL9, and vascular endothelial growth factor (VEGF). Treatment with the PI3K/mTOR dual inhibitor, NVP-BE2235, profoundly decreased secretion of all these cytokines ($P < .001$ by post-hoc Tukey test), whereas

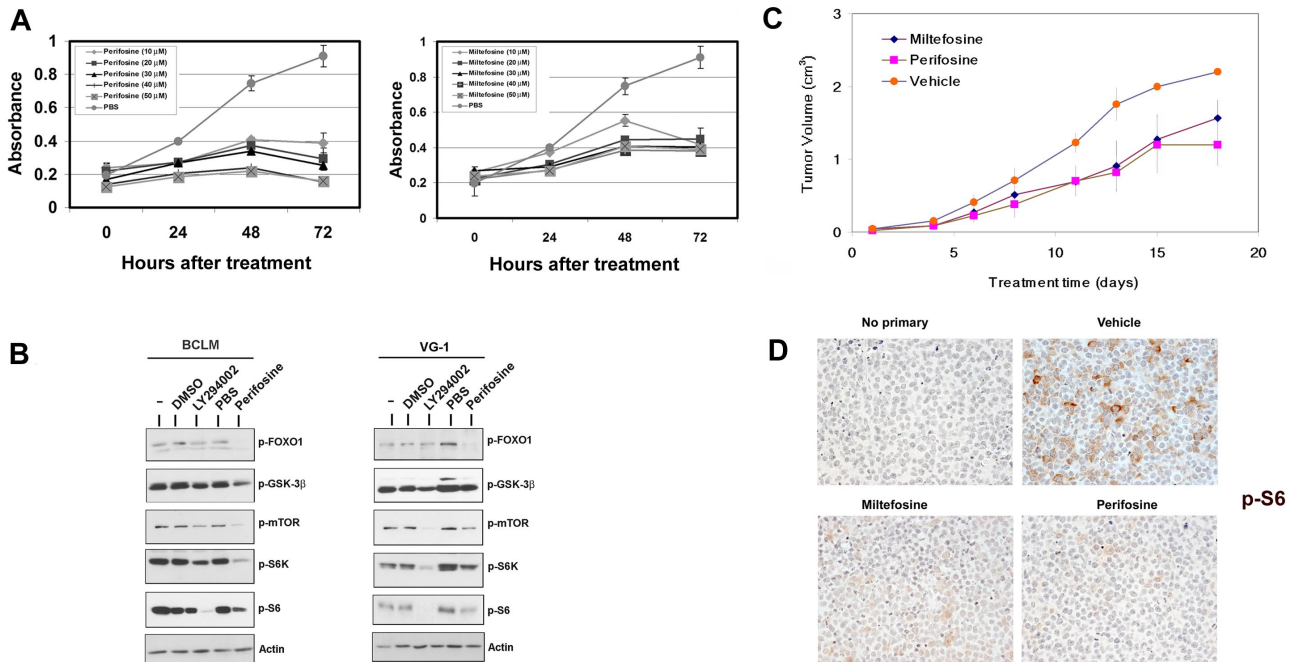


Figure 4. Effects of alkylphospholipids on PEL. (A) Inhibition of PEL cell proliferation induced by miltefosine (right panel) and perifosine (left panel) as measured by MTS assay. Shown in each panel is the absorbance at 490 nm (y-axis) in the absence of drug (gray circles) or increasing, indicated doses of either miltefosine or perifosine, ranging from 10 μ M to 50 μ M. Treatment time is represented on the x-axis. Each data point is the average of triplicate or quadruplicate measurements. Error bars represent the SD and, in most cases, are smaller than the symbol. (B) Immunoblot analysis of extracts harvested from indicated PEL cell lines treated with DMSO (vehicle), the indicated drug, or untreated cells (-). Membranes were probed with antibodies raised specifically against the phosphorylated forms of FOXO1, GSK3 β , mTOR, S6K, or S6 proteins. Membranes were probed with anti-actin antibody, as a loading control. (C) Tumor progression is delayed in miltefosine-treated mice and significantly delayed in perifosine-treated mice. Mice were treated with 50 mg/kg miltefosine (n = 5), perifosine (n = 5), or vehicle (n = 5) by intraperitoneal injection and followed for 20 days after formation of palpable tumors. Error bars represent the SD for each group of animals. (D) Tumors excised from miltefosine- and perifosine-treated mice display decreased phosphorylation of the ribosomal S6 protein, compared with vehicle controls. Staining is not observed in sections not incubated with primary antibody. Original magnification \times 400.

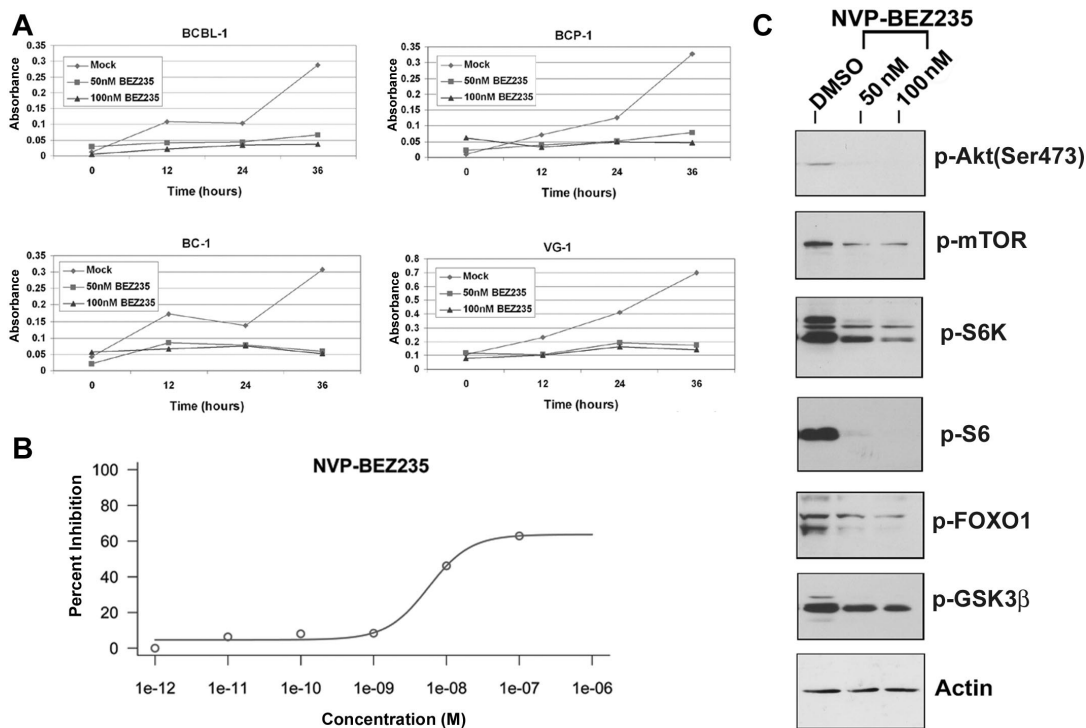


Figure 5. Low doses of NVP-BE2235 are sufficient to inhibit proliferation of PEL cells in vitro, by inhibiting the downstream targets of PI3K/mTOR pathway. (A) Inhibition of proliferation of the indicated PEL cell lines on treatment with NVP-BE2235 as measured by the MTS assay. Shown in each panel is the absorbance at 490 nm (y-axis) in the absence of drug (gray diamond) or increasing, indicated doses of NVP-BE2235. Treatment time is represented on the x-axis. Each data point is the average of triplicate or quadruplicate measurements. Error bars represent the SD and, in most cases, are smaller than the symbol. (B) The IC₅₀ curve for NVP-BE2235 showing an IC₅₀ value of 5.68 \pm 1.76nM for BC-1 PEL cells. (C) Immunoblot analysis of extracts harvested from PEL cell line treated with DMSO (vehicle) or increasing doses of NVP-BE2235. Membranes were probed with antibodies raised specifically against the phosphorylated forms of Akt (Ser473), mTOR, S6K, pS6, FOXO1, and GSK3 β . Membranes were also probed with anti-actin antibody, as a loading control.

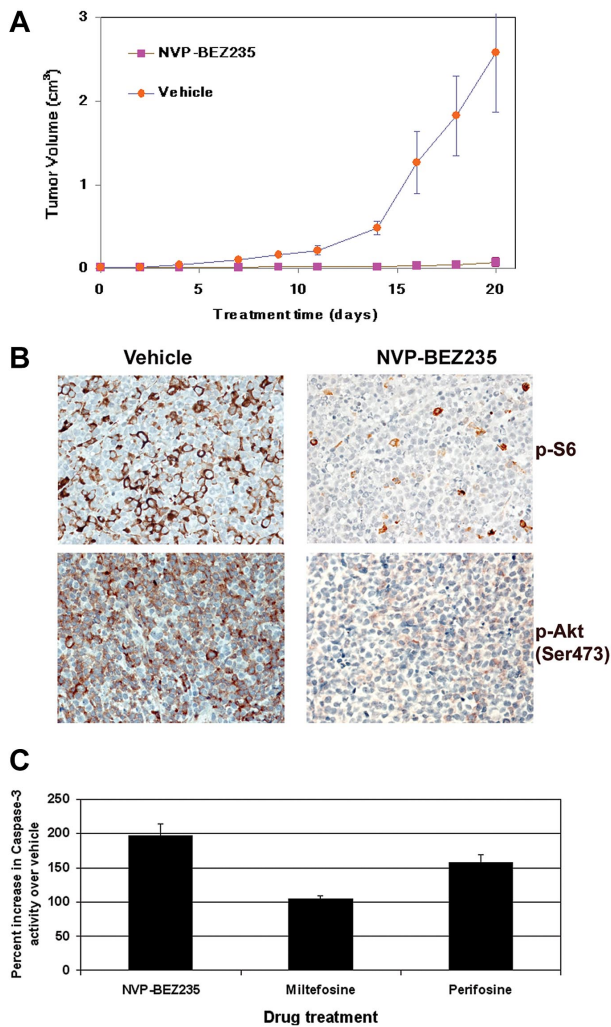


Figure 6. Treatment with NVP-BEZ235 delays tumor progression in vivo in a xenograft model of PEL. (A) Tumor progression is significantly delayed ($P < .001$) in mice treated with 40 mg/kg NVP-BEZ235 administered by oral gavage. Mice were treated 5 times per week with NVP-BEZ235 ($n = 7$) or vehicle ($n = 6$) after the development of palpable tumors. Mice were followed for 20 days, at which point vehicle-treated mice were killed. NVP-BEZ235-treated mice had significantly smaller tumors. Error bars represent the SD for each group of animals. (B) Immunohistochemical analyses reveal decreased phosphorylation of ribosomal S6 protein and Akt (Ser473) in NVP-BEZ235-treated mice. No staining was observed in sections that had not been incubated with specific antibodies. (C) PI3K/Akt inhibition induces apoptosis in PEL. A total of 1×10^6 BC-1 PEL cells were treated with 50 μ M miltefosine, 50 μ M perifosine, or 20 nM NVP-BEZ235, and the appropriate vehicle controls. Cells were harvested and lysed 12 hours later. Equivalent micrograms of cell lysate for all samples were incubated with a fluorogenic caspase-3 substrate (DEVD-AFC). Caspase-3 cleavage of the fluorescent DEVD substrate was measured on a fluorometer. The percentage of caspase-3 activity in BC-1 cells after incubation with perifosine, miltefosine, or NVP-BEZ235 was calculated compared with vehicle-treated cells. Percentage increase in caspase-3 activity of drug-treated cells compared with the respective vehicle control-treated cells is shown on the y-axis, and the specific inhibitor is shown on the x-axis.

miltefosine, perifosine, and rosiglitazone did not significantly alter the cytokine profile of PEL cells. After NVP-BEZ235 treatment for 72 hours, IL-6 and IL-10 levels were 80% lower than vehicle control-treated cells. Perifosine reduced IL-6 levels to 50% of control while minimally altering IL-10 secretion. Levels of VEGF, MIG/CXCL9, HGF, and IP-10/CXCL10 were decreased between 50% and 70% by the dual inhibitor NVP-BEZ235 compared with the control but were virtually unaffected by either perifosine or miltefosine. Interestingly, NVP-BEZ235 also reduced the transcript levels of some of the cytokines, such as VEGF (data not

shown). Activation of PI3K has previously been shown to regulate VEGF transcription,³⁸ and hence dual inhibition of PI3K and mTOR likely affects both mRNA transcript and protein levels of some of these cytokines. Curiously, rosiglitazone dramatically reduced the levels of IP-10 and HGF, similar to that seen with NVP-BEZ235 treatment, without affecting the secretion levels of any other assayed cytokines. The difference in cytokine profile expression between NVP-BEZ235-treated cells and those treated with the other inhibitors separates the in vitro proliferation inhibition phenotype from the tumor growth inhibition seen in vivo. Although all the inhibitors could prevent proliferation in vitro, NVP-BEZ235 was most efficacious at inhibiting tumor growth in vivo, probably because of the inhibition of multiple autocrine and paracrine growth factors.

Discussion

We and others have previously shown that individual KSHV viral proteins, such as K1 and vGPCR, activate the PI3K/Akt/mTOR pathway in B cells and endothelial cells.¹²⁻¹⁶ KSHV-infected PELs also display constitutive high-level activation of the PI3K/Akt/mTOR pathway.¹⁰ Our findings indicate that inhibiting this pathway is an effective modality for treating PEL.

We determined that the glitazone class of drugs, which are known to activate AMPK, have limited efficacy. Ciglitazone and rosiglitazone induced dose-dependent inhibition of PEL growth in vitro. This correlated with AMPK activation and mTOR inhibition. Although effective in culture, AMPK activation by rosiglitazone only marginally reduced tumor growth in a xenograft model of PEL.

Miltefosine and perifosine are direct inhibitors of Akt. Both induced dose-dependent inhibition of PEL in culture and also inhibited the downstream targets of Akt, such as mTOR, leading to reduced phosphorylation and activation of S6K and S6. Importantly, they also inhibited Akt targets that are not part of the mTOR pathway, eg, FOXO1, and are therefore expected to have a greater therapeutic impact than mTORC1 inhibitors alone. In our PEL xenograft model, perifosine reduced tumor volume and growth to a statistically significant extent, compared with vehicle-treated mice. These 2 compounds therefore warrant further study for the treatment of PEL.

The dual PI3K/mTOR inhibitor NVP-BEZ235^{35,36} was more effective than compounds that targeted only a single member of the PI3K/Akt/mTOR pathway. Our results demonstrate that the PI3K/mTOR dual inhibitor NVP-BEZ235 effectively inhibited the proliferation of PEL cell lines in vitro at a very low IC_{50} of 5.68 plus or minus 1.76 nM.

NVP-BEZ235 efficacy was comparable across all PEL cell lines tested, even those that showed partial resistance to rapamycin,¹⁰ and was independent of p53 mutation status. BCBL-1, BC-1, BCP-1, and VG-1 showed comparable inhibition of proliferation, suggesting that dual inhibition of PI3K and mTOR negates any survival advantage conferred by p53 mutations present in PEL cell lines.

The selective activity of NVP-BEZ235 on PI3K and mTOR was demonstrated by reduced phosphorylation of their downstream targets. Reduced phosphorylation of FOXO1 and GSK3 β , the downstream targets of Akt, confirmed the inhibition of PI3K, whereas reduced phosphorylation of S6K and ribosomal S6 confirmed inhibition of mTOR. Importantly, there was an inhibition of phosphorylation of Akt at Ser473. This site is phosphorylated by the rapamycin-insensitive mTORC2, which is responsible for activating Akt in a feedback loop and has been implicated in rapamycin failure after prolonged treatment.^{39,40} NVP-BEZ235 can prevent this feedback loop.

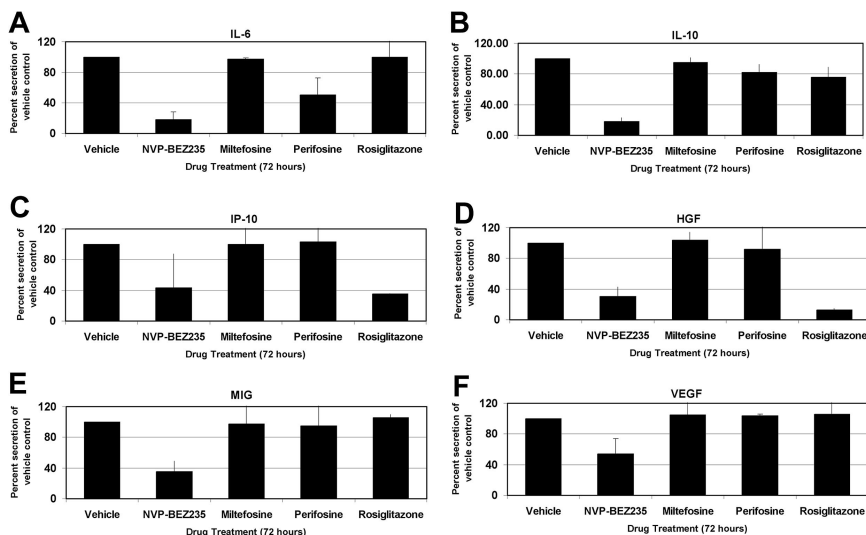


Figure 7. Profile of cellular cytokine levels after inhibition of PI3K/Akt/mTOR pathway members. IL-6 (A), IL-10 (B), IP-10 (C), HGF (D), MIG (E), and VEGF (F) levels on treatment with indicated compounds or with vehicle control. Changes in cytokine levels are represented as percentage change from vehicle-treated levels, which were set to 100%. Error bars represent SD. The PI3K/mTOR dual inhibitor NVP-BE2235 dramatically reduces levels of the indicated cytokines secreted into the growth medium. $P < .001$ by Tukey post-hoc test.

NVP-BE2235 significantly ($P < .001$) reduced tumor growth in our PEL xenograft model. Tumors excised from NVP-BE2235-treated mice displayed reduced phosphorylation of both ribosomal S6 protein and Akt (Ser473), confirming *in vivo* inhibition of its targets. Importantly, this compound is orally bioavailable, making it an attractive therapeutic molecule. Furthermore, NVP-BE2235 treatment induced higher levels of apoptosis in PEL cells, as measured by caspase-3 activity, compared with the other PI3K/Akt inhibitors.

PEL is characterized by elevated IL-6 and IL-10 cytokine secretion.³⁷ Our group has previously demonstrated that IL-10 may be used as a prognostic marker of PEL, and we have demonstrated that rapamycin treatment reduces IL-6 and IL-10 secretion in culture and *in vivo*.¹⁰ Using Luminex bead-based technology, we investigated the secretion profile of many cytokines after treatment with each of the compounds described in this study, or with the appropriate vehicle control. Six cytokines (IL-6, IL-10, IP-10, HGF, MIG, and VEGF) were secreted to high levels in the growth medium of BC-1 cells consistent with earlier observations.^{41,42} NVP-BE2235 dramatically reduced secretion of all these cytokines 72 hours after treatment. The other Akt/mTOR pathway inhibitors exhibited weaker, more differential phenotypes. Rosiglitazone significantly reduced secretion of IP-10 and HGF but only modestly decreased IL-10 secretion, whereas all other cytokine profiles remained unaltered. The Akt inhibitor perifosine reduced IL-6 secretion by 50%, and that of IL-10 by 20%.

Only NVP-BE2235 inhibited VEGF. VEGF is an angiogenic growth factor that is involved in tumor proliferation.⁴³ HGF has been implicated in tumorigenesis of diffuse large B-cell lymphomas and has been shown to activate Akt through PI3K.⁴⁴ CXCL10/IP-10 and CXCL9/MIG are chemokines that attract T lymphocytes and appear to antagonize angiogenesis.⁴⁵ However, these chemokines also play a role in B lymphocyte migration and dissemination.⁴⁶ In addition, unlike normal B lymphocytes, Hodgkin lymphoma and several different types of NHL, including chronic lymphocytic leukemia, small lymphocytic lymphoma, follicular lymphoma, marginal zone B-cell lymphoma, and mantle cell lymphoma,^{47,48} have been reported to express CXCL9/MIG and CXCL10/IP-10 and their cognate receptor CXCR3 as part of an autocrine loop. We surmise that these cytokines, chemokines, and growth factors play an important role in NHL in general and that our results may therefore be applicable to other NHLs beyond PEL.

In conclusion, the PI3K/Akt/mTOR axis is an important target in NHL because it regulates cell survival, protein translation, and, as we show here, cytokine production. Dual inhibition of the PI3K

and mTOR kinases inhibits the translation and secretion of the essential paracrine and autocrine cytokines required for growth. This is in addition to cell-intrinsic mTOR targets, such as myc and cyclin D1.⁴⁹ Inhibition of these cytokines is required for inhibiting PEL tumor growth *in vivo*. Thus, this dual inhibitor may prove therapeutic for tumors that are critically dependent on autocrine and paracrine growth factors for their survival.

Acknowledgments

The authors thank Novartis for providing us with NVP-BE2235, Tatiana Quintero-Matthews for her technical expertise, the Clinical Proteomics Laboratory of the University of North Carolina Thurston Arthritis Research Center, Charlene Ross and the Animal Studies core for their help, S. Krown for manuscript proofreading, and members of the Damania and Dittmer laboratories for helpful discussions.

B.D. is a Leukemia & Lymphoma Society Scholar, American Heart Association established investigator, and a Burroughs Wellcome Fund Investigator in Infectious Disease. This work was supported by the National Institutes of Health (grant CA096500), University Cancer Research Fund and University of Pennsylvania (CFAR pilot project grant P30-AI045008; B.D.), as well as the Leukemia & Lymphoma Society (6021), the AIDS malignancy consortium (CA121947), and the National Institutes of Health (CA DE018304; D.P.D.). A.P.B. was supported by Cancer Cell Biology (training grant T32CA071341).

Authorship

Contribution: A.P.B. and P.M.B. designed and performed experiments, analyzed results, and wrote the manuscript; S.-H.S. and D.R. helped with experiments; D.P.D. performed statistical analysis and provided critical input; and B.D. designed experiments, analyzed results, and wrote the manuscript.

Conflict-of-interest disclosure: The authors declare no competing financial interests.

Correspondence: Blossom Damania, Lineberger Comprehensive Cancer Center, CB#7295, University of North Carolina, Chapel Hill, NC 27599; e-mail: damania@med.unc.edu.

References

- Cross DA, Alessi DR, Cohen P, Andjelkovich M, Hemmings BA. Inhibition of glycogen synthase kinase-3 by insulin mediated by protein kinase B. *Nature*. 1995;378(6559):785-789.
- Datta SR, Dudek H, Tao X, et al. Akt phosphorylation of BAD couples survival signals to the cell-intrinsic death machinery. *Cell*. 1997;91(2):231-241.
- del Peso L, Gonzalez-Garcia M, Page C, Herrera R, Nunez G. Interleukin-3-induced phosphorylation of BAD through the protein kinase Akt. *Science*. 1997;278(5338):687-689.
- Cardone MH, Roy N, Stennicke HR, et al. Regulation of cell death protease caspase-9 by phosphorylation. *Science*. 1998;282(5392):1318-1321.
- Manning BD, Cantley LC. AKT/PKB signaling: navigating downstream. *Cell*. 2007;129(7):1261-1274.
- Shaw RJ, Bardeesy N, Manning BD, et al. The LKB1 tumor suppressor negatively regulates mTOR signaling. *Cancer Cell*. 2004;6(1):91-99.
- Fryer LG, Parbu-Patel A, Carling D. The anti-diabetic drugs rosiglitazone and metformin stimulate AMP-activated protein kinase through distinct signaling pathways. *J Biol Chem*. 2002;277(28):25226-25232.
- Panigrahy D, Singer S, Shen LQ, et al. PPAR-gamma ligands inhibit primary tumor growth and metastasis by inhibiting angiogenesis. *J Clin Invest*. 2002;110(7):923-932.
- Gimun GD, Naseri E, Vafai SB, et al. Synergy between PPARgamma ligands and platinum-based drugs in cancer. *Cancer Cell*. 2007;11(5):395-406.
- Sin SH, Roy D, Wang L, et al. Rapamycin is efficacious against primary effusion lymphoma (PEL) cell lines in vivo by inhibiting autocrine signaling. *Blood*. 2007;109(5):2165-2173.
- Boulanger E, Gerard L, Gabarre J, et al. Prognostic factors and outcome of human herpesvirus 8-associated primary effusion lymphoma in patients with AIDS. *J Clin Oncol*. 2005;23(19):4372-4380.
- Wang L, Damania B. Kaposi's sarcoma-associated herpesvirus confers a survival advantage to endothelial cells. *Cancer Res*. 2008;68(12):4640-4648.
- Tomlinson CC, Damania B. The K1 protein of Kaposi's sarcoma-associated herpesvirus activates the Akt signaling pathway. *J Virol*. 2004;78(4):1918-1927.
- Tomlinson CC, Damania B. Critical role for endocytosis in the regulation of signaling by the Kaposi's sarcoma-associated herpesvirus K1 protein. *J Virol*. 2008;82(13):6514-6523.
- Wang L, Wakisaka N, Tomlinson CC, et al. The Kaposi's sarcoma-associated herpesvirus (KSHV/HHV8) K1 protein induces expression of angiogenic and invasion factors. *Cancer Res*. 2004;64(8):2774-2781.
- Wang L, Dittmer DP, Tomlinson CC, Fakhari FD, Damania B. Immortalization of primary endothelial cells by the K1 protein of Kaposi's sarcoma-associated herpesvirus. *Cancer Res*. 2006;66(7):3658-3666.
- Bais C, Van Geelen A, Eroles P, et al. Kaposi's sarcoma associated herpesvirus G protein-coupled receptor immortalizes human endothelial cells by activation of the VEGF receptor-2/ KDR. *Cancer Cell*. 2003;3(2):131-143.
- Sodhi A, Montaner S, Patel V, et al. Akt plays a central role in sarcomagenesis induced by Kaposi's sarcoma herpesvirus-encoded G protein-coupled receptor. *Proc Natl Acad Sci U S A*. 2004;101(14):4821-4826.
- Sodhi A, Chaisuparat R, Hu J, et al. The TSC2/mTOR pathway drives endothelial cell transformation induced by the Kaposi's sarcoma-associated herpesvirus G protein-coupled receptor. *Cancer Cell*. 2006;10(2):133-143.
- Montaner S, Sodhi A, Pece S, Mesri EA, Gutkind JS. The Kaposi's sarcoma-associated herpesvirus G protein-coupled receptor promotes endothelial cell survival through the activation of Akt/protein kinase B. *Cancer Res*. 2001;61(6):2641-2648.
- Sodhi A, Montaner S, Patel V, et al. The Kaposi's sarcoma-associated herpes virus G protein-coupled receptor up-regulates vascular endothelial growth factor expression and secretion through mitogen-activated protein kinase and p38 pathways acting on hypoxia-inducible factor 1alpha. *Cancer Res*. 2000;60(17):4873-4880.
- Boulanger E, Marchio A, Hong SS, Pineau P. Mutational analysis of TP53, PTEN, PIK3CA and CTNNB1/beta-catenin genes in human herpesvirus 8-associated primary effusion lymphoma. *Haematologica*. 2009;94(8):1170-1174.
- Jacinto E, Loewith R, Schmidt A, et al. Mammalian TOR complex 2 controls the actin cytoskeleton and is rapamycin insensitive. *Nat Cell Biol*. 2004;6(11):1122-1128.
- Faraway JJ. *Extending the Linear Model With R*. Boca Raton, FL: Chapman and Hall/CRC; 2006.
- Inoki K, Zhu T, Guan KL. TSC2 mediates cellular energy response to control cell growth and survival. *Cell*. 2003;115(5):577-590.
- Inoki K, Ouyang H, Zhu T, et al. TSC2 integrates Wnt and energy signals via a coordinated phosphorylation by AMPK and GSK3 to regulate cell growth. *Cell*. 2006;126(5):955-968.
- Ruiter GA, Zerp SF, Bartelink H, van Blitterswijk WJ, Verheij M. Anti-cancer alkyl-lysophospholipids inhibit the phosphatidylinositol 3-kinase-Akt/PKB survival pathway. *Anticancer Drugs*. 2003;14(2):167-173.
- LoPiccolo J, Blumenthal GM, Bernstein WB, Dennis PA. Targeting the PI3K/Akt/mTOR pathway: effective combinations and clinical considerations. *Drug Resist Updat*. 2008;11(1):32-50.
- Yamauchi T, Waki H, Kamon J, et al. Inhibition of RXR and PPARgamma ameliorates diet-induced obesity and type 2 diabetes. *J Clin Invest*. 2001;108(7):1001-1013.
- Han S, Roman J. Rosiglitazone suppresses human lung carcinoma cell growth through PPAR-gamma-dependent and PPARgamma-independent signal pathways. *Mol Cancer Ther*. 2006;5(2):430-437.
- Heaney AP, Fernando M, Yong WH, Melmed S. Functional PPAR-gamma receptor is a novel therapeutic target for ACTH-secreting pituitary adenomas. *Nat Med*. 2002;8(11):1281-1287.
- Petre CE, Sin SH, Dittmer DP. Functional p53 signaling in Kaposi's sarcoma-associated herpesvirus lymphomas: implications for therapy. *J Virol*. 2007;81(4):1912-1922.
- Okoshi R, Ozaki T, Yamamoto H, et al. Activation of AMP-activated protein kinase induces p53-dependent apoptotic cell death in response to energetic stress. *J Biol Chem*. 2008;283(7):3979-3987.
- Hideshima T, Catley L, Yasui H, et al. Perifosine, an oral bioactive novel alkylphospholipid, inhibits Akt and induces in vitro and in vivo cytotoxicity in human multiple myeloma cells. *Blood*. 2006;107(10):4053-4062.
- Maira SM, Stauffer F, Brueggen J, et al. Identification and characterization of NVP-BEZ235, a new orally available dual phosphatidylinositol 3-kinase/mammalian target of rapamycin inhibitor with potent in vivo antitumor activity. *Mol Cancer Ther*. 2008;7(7):1851-1863.
- Serra V, Markman B, Scaltriti M, et al. NVP-BEZ235, a dual PI3K/mTOR inhibitor, prevents PI3K signaling and inhibits the growth of cancer cells with activating PI3K mutations. *Cancer Res*. 2008;68(19):8022-8030.
- Aoki Y, Yarchoan R, Braun J, Iwamoto A, Tosato G. Viral and cellular cytokines in AIDS-related malignant lymphomatous effusions. *Blood*. 2000;96(4):1599-1601.
- Kang J, Rychahou PG, Ishola TA, Mourou JM, Evers BM, Chung DH. N-myc is a novel regulator of PI3K-mediated VEGF expression in neuroblastoma. *Oncogene*. 2008;27(28):3999-4007.
- Bayascas JR, Alessi DR. Regulation of Akt/PKB Ser473 phosphorylation. *Mol Cell*. 2005;18(2):143-145.
- Sarbasov DD, Guertin DA, Ali SM, Sabatini DM. Phosphorylation and regulation of Akt/PKB by the rictor-mTOR complex. *Science*. 2005;307(5712):1098-1101.
- Drexler HG, Meyer C, Gaidano G, Carbone A. Constitutive cytokine production by primary effusion (body cavity-based) lymphoma-derived cell lines. *Leukemia*. 1999;13(4):634-640.
- Capello D, Gaidano G, Gallicchio M, et al. The tyrosine kinase receptor met and its ligand HGF are co-expressed and functionally active in HHV-8 positive primary effusion lymphoma. *Leukemia*. 2000;14(2):285-291.
- Lohela M, Bry M, Tammela T, Alitalo K. VEGFs and receptors involved in angiogenesis versus lymphangiogenesis. *Curr Opin Cell Biol*. 2009;21(2):154-165.
- Tjin EP, Groen RW, Vogelzang I, et al. Functional analysis of HGF/MET signaling and aberrant HGF-activator expression in diffuse large B-cell lymphoma. *Blood*. 2006;107(2):760-768.
- Sgadari C, Farber JM, Angiolillo AL, et al. Mig, the monokine induced by interferon-gamma, promotes tumor necrosis in vivo. *Blood*. 1997;89(8):2635-2643.
- Pals ST, de Gorter DJ, Spaargaren M. Lymphoma dissemination: the other face of lymphocyte homing. *Blood*. 2007;110(9):3102-3111.
- Teichmann M, Meyer B, Beck A, Niedobitek G. Expression of the interferon-inducible chemokine IP-10 (CXCL10), a chemokine with proposed anti-neoplastic functions, in Hodgkin lymphoma and nasopharyngeal carcinoma. *J Pathol*. 2005;206(1):68-75.
- Jones D, Benjamin RJ, Shahsafaei A, Dorfman DM. The chemokine receptor CXCR3 is expressed in a subset of B-cell lymphomas and is a marker of B-cell chronic lymphocytic leukemia. *Blood*. 2000;95(2):627-632.
- Gera JF, Mellingshoff IK, Shi Y, et al. AKT activity determines sensitivity to mammalian target of rapamycin (mTOR) inhibitors by regulating cyclin D1 and c-myc expression. *J Biol Chem*. 2004;279(4):2737-2746.